

Flexible foils with electrochromic coatings: science, technology and applications

A. Azens^a, E. Avendaño^a, J. Backholm^a,
L. Berggren^a, G. Gustavsson^b, R. Karmhag^b,
G.A. Niklasson^a, A. Roos^a, C.G. Granqvist^{a,*}

^a Department of Engineering Sciences, The Ångström Laboratory, Uppsala University, P.O. Box 534, SE-75121 Uppsala, Sweden

^b ChromoGenics Sweden AB, c/o Uppsala University Holding, SE-75183 Uppsala, Sweden.

Received 20 April 2004; received in revised form 16 May 2004; accepted 9 December 2004

Abstract

This paper covers a number of aspects of a novel flexible electrochromic foil capable of varying its optical transmittance. The foil includes thin films of tungsten oxide and nickel oxide and an intervening polymer electrolyte serving as lamination material. Concerning *scientific* aspects, we discuss the prevalent defects in amorphous tungsten oxide and how they lead to a consistent picture of the optical properties of tungsten oxide films as a function of non-stoichiometry and ion intercalation. We also present a refined model for the coloration/bleaching due to proton extraction/insertion in surface sheaths of nano-crystallites of nickel oxide. We then turn to aspects of *technology* and treat ways to enhance the bleached-state transmittance by mixing the nickel oxide with another oxide having a wide band gap, pre-assembly charge insertion/extraction by facile gas treatments of the films and practical device manufacturing. The final part covers some *applications* with emphasis on architectural “smart windows” capable of achieving improved indoor comfort together with significant energy savings due to lowered demands for space cooling. We also touch upon applications concerning eyewear.

© 2005 Elsevier B.V. All rights reserved.

Keywords: Electrochromic properties; Tungsten trioxide; Nickel oxide; Optical properties

1. Introduction

Electrochromic materials are able to reversibly change their optical properties upon charge insertion/extraction induced by an external voltage [1–3]. The materials can be integrated in electrochromic devices of several different types, which can be all-solid-state constructions as well as polymer laminated ones, with or without self-powering by solar cells [4]. These devices open a number of technologically interesting possibilities to modulate optical transmittance, reflectance, absorptance and emittance. Recently, special attention has been devoted to designs incorporating electrochromic hydrated nickel oxide films operating in conjunc-

tion with electrochromic tungsten oxide. This combination of materials is favorable with regard to electrochemical potentials and also for the possibility to attain a neutral gray color in the dark state. Rigid (usually glass-based) devices [5–17] as well as flexible, polyester-based foil devices [3,9,18] have been investigated during the last decade.

Among the numerous applications of electrochromism, we note architectural “smart windows”, which are able to combine improved indoor comfort (less glare and thermal stress) with good energy efficiency (especially lowered air conditioning loads in cooled buildings) [18]. The use of “smart windows” has been discussed in some detail in literature on innovative architecture [19,20]. Other applications concern non-emissive displays, variable-reflectance mirrors, variable-transmittance eyewear for a variety of applications and variable-emittance surfaces for temperature stabilization of space vehicles.

* Corresponding author. Tel.: +46 18 471 3067; fax: +46 18 500 131.

E-mail addresses: Greger.Gustavsson@angstrom.uu.se (G. Gustavsson), claes-goran.granqvist@angstrom.uu.se (C.G. Granqvist).

The object of this paper is to summarize a number of state-of-the-art issues with regard to electrochromic foil devices incorporating cathodically coloring tungsten oxide and anodically coloring nickel oxide. We cover some aspects related to science, technology and applications with focus on developments that have taken place during the recent past.

2. Scientific aspects

Our understanding of basic features of the electrochromism in tungsten oxide and nickel oxide have progressed significantly during the past few years. We first introduce the main defects believed to prevail in amorphous tungsten oxide films and then demonstrate that these defects lead to a conceptually simple framework for reconciling a large body of optical data for films with varying stoichiometry and level of ion intercalation. We then turn to nickel oxide and a refinement of the conventional model for electrochromic coloration and bleaching.

2.1. Defect states in amorphous tungsten oxide

We discuss tungsten oxide following recent work by Niklasson et al. [21]. This material is based on corner-sharing WO_6 octahedra. They are perfectly ordered in the WO_3 single crystal but subject to variation in bond angle and bond length in the “amorphous” state characteristic for electrochromic films [1]. Stoichiometric WO_3 is basically an ionic solid comprising W^{6+} and O^{2-} ions, although there is also some covalency [22]. The valence and conduction bands are based on $\text{O}2p$ and $\text{W}5d$ orbitals, respectively. Each tungsten ion is surrounded by six oxygen ions forming an octahedron; each oxygen ion is bound to two tungsten ions in a linear configuration according to $\text{W}^{6+}-\text{O}^{2-}-\text{W}^{6+}$.

Tungsten oxide has a propensity to form sub-stoichiometric structures, manifested in the crystalline state as the Magnéli phases. In amorphous structures, the most common defect is the *oxygen vacancy*, which can be neutral (V^0), singly charged (V^+) or doubly charged (V^{2+}). A neutral vacancy has an electron concentration similar to that of the stoichiometric compound, but it is energetically favorable to transfer one or both of its electrons to neighboring tungsten ions. When one electron is transferred, the situation can be represented as $\text{W}^{5+}-\text{V}^+-\text{W}^{6+}$. The electron transferred to the W^{5+} site enters the conduction band of tungsten oxide. Considering V^{2+} , the two electrons can be transferred to one or two adjacent tungsten ions. The former of these cases will lead to the formation of W^{4+} . We note in this connection that optical absorption due to transitions between W^{4+} and W^{5+} states has been proposed as being the origin of electrochromism in tungsten oxide [23–25]. This model is problematical, though, and W^{4+} states appear to be energetically unfavorable [26]; they have been verified by X-ray photoelectron spectroscopy only at O/W ratios as small as ~ 2.6 and below [27]. It is energetically more advantageous

to form V^{2+} along with two W^{5+} ions. The electron–phonon interaction is strong in tungsten oxide so that structural rearrangements can occur easily with tungsten ions approaching each other, implying that doubly charged $(\text{W}-\text{W})^{10+}$ complexes are formed. Recent band structure calculations have identified the existence of such complexes and have shown that the extra electrons occupy states deep in the band gap [26,28]; these states are obviously occupied by two electrons and hence filled. It is interesting to note that the formation of the $(\text{W}-\text{W})^{10+}$ complexes can be seen as a manifestation of Anderson localization [29], which is pronounced as a consequence of the strong electron–phonon interaction. We expect that V^{2+} is the most common type of vacancy in tungsten oxide.

Oxygen over-stoichiometry is possible in tungsten oxide, at least when produced by sputter deposition [30]. This excess of oxygen can be accommodated if there are hydroxyl bonds between adjacent oxygen atoms as illustrated, highly schematically, by $\text{W}^{6+}-\text{(O-O)}^{2-}-\text{W}^{6+}$. The extra oxygen atoms can be viewed as *oxygen interstitials*; they can be neutral or singly or doubly charged as a result of electron trapping [31]. There is no fundamental reason against vacancies and interstitials being present simultaneously in tungsten oxide films.

Electrochromism in tungsten oxide is induced by *intercalation of small ions*, typically being H^+ or Li^+ . Specifically, we regard H^+ since the foil devices discussed below rely mainly on proton transport. The insertion of H^+ breaks up the continuous $\text{W}-\text{O}-\text{W}$ network to form structures of the type $\text{W}^{6+}-\text{O}^{2-}-\text{H}^+$ (W^{5+}). In a schematic chemical picture, the hydrogen ion is bound to an oxygen ion while its outer electron is transferred to a neighboring tungsten site thereby forming W^{5+} . This is analogous to the case of V^+ discussed above, i.e., the electron enters the conduction band of tungsten oxide.

2.2. Optical properties of amorphous tungsten oxide films

This section discusses the optical properties of tungsten oxide films having defect structures as discussed above. The films were prepared by sputter deposition and subsequent voltammetric cycling to ensure reversible properties under conditions that were specified elsewhere [32,33].

Stoichiometric WO_3 films are transparent for energies below the fundamental band gap at ~ 3 eV, and ion intercalation leads to electrochromism manifested in a broad absorption band centered at ~ 1.2 eV, which produces a distinctly blue color [1]. An early model described this phenomenon in terms of intervalency charge transfer with electrons transferred from a W^{5+} site to an adjacent W^{6+} site [34]. This model has since been refined by introducing the polaron concept [35], and quantitative fits to experimental data have been achieved by accounting for transitions between localized states in a Gaussian density of states [32,36]. Hence, it appears that electrochromism in tungsten oxide is firmly

linked to the existence of W^{5+} sites (an alternative model presuming transitions between W^{4+} and W^{5+} [23–25] was commented upon above).

Slightly sub-stoichiometric tungsten oxide films are transparent, whereas a blue color appears in films characterized by a well-defined and narrow range of larger oxygen deficiency [37]. Fig. 1 shows recent data on the absorption coefficient α for as-deposited films of $WO_{2.89}$ and $WO_{2.63}$ [21]. The W/O ratio was determined by elastic recoil detection analysis (ERDA) and is reliable to ± 0.03 . The former film is transparent whereas the latter one shows prominent polaron absorption similar to that in an ion intercalated $WO_{2.89}$ film. Recent electrochemical experiments showed that the demarcation between transparent and blue as-deposited films lies at W/O ratios between 2.75 and 2.8. These data can be reconciled with the defect model outlined above. The strong electron–phonon coupling tends to favor the formation of $(W-W)^{10+}$ complexes, which do not lead to optical absorption. However, singly charged oxygen vacancies yield absorption due to intervalence charge transfer. The analogy with data for the ion intercalated film is expected since W^{5+} sites are present in both cases. It thus appears that amorphous tungsten oxide films display a cross-over from defects with paired electrons—according to the Anderson mechanism—and singly charged oxygen vacancies as the density of vacancies is increased, but the underlying causes for this interesting behavior are not clear.

We next consider over-stoichiometric tungsten oxide films and first note that initial Li^+ intercalation is irreversible and does not lead to coloration, which has been attributed to formation of strongly bound Li_2O complexes [30,38]. Furthermore, irreversibility in the charge insertion is

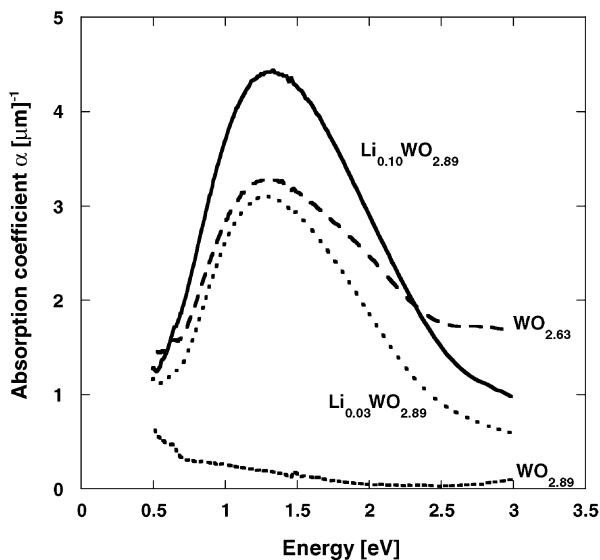


Fig. 1. Optical absorption coefficient vs. energy for two as-deposited amorphous tungsten oxide films with the shown stoichiometries. Two spectra for different levels of Li^+ intercalation into the initially transparent film are also shown for comparison.

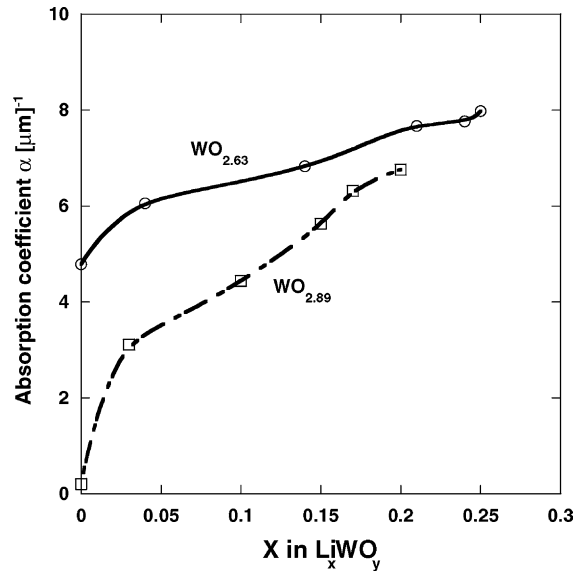


Fig. 2. Optical absorption coefficient vs. Li/W ratio x for the two amorphous tungsten oxide films reported on in Fig. 1. The shown absorption coefficients represent maxima in the spectra.

commonly found during the first color/bleach cycles, and the films remain transparent up to a threshold of inserted charge where coloration sets in whereas subsequent cycles are reversible so that electrochromism prevails [39]. Again the explanation is likely to lie in Li_2O formation in films containing oxygen interstitials, and a similar mechanism may account for the at first sight curious fact that some tungsten oxide films prepared by sputtering under oxygen-rich conditions can be colored by Li^+ insertion but not bleached again [21].

Ion intercalation into tungsten oxide films leads to a gradual increase of α , which can be associated with a growth of the number of W^{5+} sites, as pointed out above. For increasing intercalation in a reversible color/bleach cycle, there is initially a proportionality between α and the density of ions, but subsequently the increase slows down and the absorption attains a maximum for a Li/W ratio of 0.3–0.5 [32,40] and α then starts to drop. This can be understood, schematically, as a decrease in the density of W^{6+} final states available for intervalence charge transfer [40].

It was noted in the discussion around Fig. 1 that the absorption in sub-stoichiometric blue tungsten oxide films was very similar to the one in Li^+ intercalated film. We next consider the evolution of optical absorption as Li^+ is inserted into blue sub-stoichiometric films. Fig. 2 shows that α increases more gradually than in less sub-stoichiometric and initially transparent films. These observations can be reconciled with the notions put forward above. The intercalated ion can bind to oxygen ions or to singly charged oxygen vacancies. The second alternative does not lead to additional optical absorption. If all singly charged oxygen vacancies have bonds to the inserted ions, there will be one W^{5+} site per Li^+ ion just as in a film without singly charged oxygen vacancies.

2.3. Coloration mechanism for nickel oxide films

Nickel oxide films have electrochromic properties with NiO and Ni(OH)₂ being visually transparent and over-stoichiometric nickel oxide (i.e., NiOOH and/or Ni₂O₃) exhibiting a dark color. The detailed coloration mechanism in electrochromic nickel oxide has been debated for a long time [1], and new experiments were carried out recently by X-ray photoemission spectroscopy (XPS) and by the galvanometric intermittent titration technique (GIT) in order to clarify the situation [41–43]. These experiments were conducted on films made by magnetron sputtering from a non-magnetic target of Ni(93%)–V(7%), as described elsewhere, and the films were electrochemically cycled to attain stable conditions [44,45]. The films were investigated by Extended X-ray absorption fine structure spectroscopy (EXAFS), and it appeared that the vanadium atoms substituted nickel in a NiO-type structure, i.e., that nickel and vanadium formed a mixed-oxide phase in the film [46].

XPS data were recorded by use of the MAXLAB synchrotron radiation facility in Lund, Sweden, using a 1.56-GeV storage ring. The photon energy was varied between 50 and 1500 eV. The end of the beam-line used a high-resolution electron analyzer having an energy resolution from 10³ to 10⁴ and a photon flux on the sample in the range of 10¹¹–10¹³ photons s⁻¹. Half of the measured sample was colored and the other half was bleached. The data were compared with published values for the binding energies of different nickel oxides [47–50]. Fig. 3 shows an XPS spectrum for the Ni2p states of such a film. The changes in the Ni2p core level suggest that the coloration is due to a transition Ni²⁺ → Ni³⁺. The broad peak at 856 eV can be interpreted as the contributions from NiO and Ni(OH)₂ for the bleached state and from NiO, Ni₂O₃ and/or NiOOH for the colored state. Nothing but NiO was detected by X-ray diffraction, and hence it can be concluded that Ni₂O₃ and/or NiOOH as well as Ni(OH)₂ are present in surface sheaths of nickel oxide nano-crystallites.

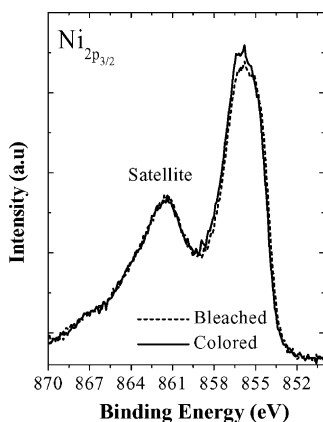


Fig. 3. XPS signal for Ni2p core levels of a nickel–vanadium oxide film colored and bleached in 1 M KOH. A photon energy of 1061 eV, with an energy pass of 75 eV and energy step of 0.1 eV, was used.

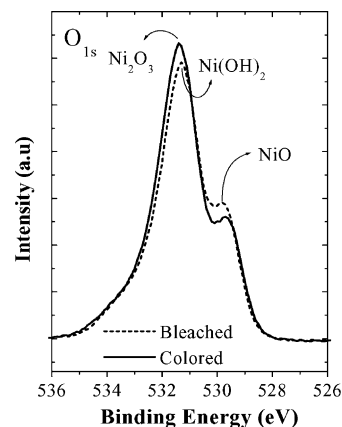
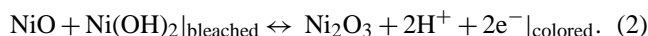
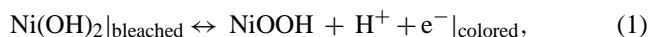


Fig. 4. XPS signal for the O1s levels of a nickel–vanadium oxide film colored and bleached in 1 M KOH. A photon energy of 1061 eV, with an energy pass of 40 eV and energy step of 0.1 eV, was used.

Oxygen-related XPS features are shown in Fig. 4; they appear around 531.2 and 530.0 eV for the bleached state and around 531.5 and 529.7 eV for the colored state. The tail around 533 eV may be a contribution from water absorbed and/or adsorbed by the film. The region around 530 eV is dominated by NiO, while Ni(OH)₂, NiOOH and Ni₂O₃ dominate in the region around 531 eV.

Upon coloration, the Ni(OH)₂-type material must lose its hydrogen and rearrange its electronic state, thereby producing the optically absorbing phase of nickel oxy-hydroxide. The shift of the Ni(OH)₂ peak at 531.2 eV to higher binding energy corresponds to a change of the valence state from 2+ to 3+ [51]. The peculiar change in the intensity around 530 eV is assigned to NiO. It does not have any H⁺ to be extracted, but it is changing its valence from 2+ to 3+. It is well known that an excess of oxygen in NiO produces a Ni²⁺ vacancy that is compensated by the creation of a hole on two Ni²⁺ sites thus producing Ni³⁺ [52]. In the present case, the extraction of H⁺ from NiOOH is compensated by the creation of one hole on the Ni²⁺ ion of NiO. The change in the area of the NiO peak is equal to the area added to the second peak, which supports the mechanism described above. The mechanism of coloration can then be expressed as the cooperative effect of the reactions



No shift of the vanadium 2p states was detectable upon coloration. A further analysis of these results will be given elsewhere [42]. It should be emphasized again that the XPS technique is surface sensitive, implying that the reactions shown above are expected to take place only on the outermost parts of the NiO-type nano-crystallites.

3. Technology

We now focus on a specific design of a flexible electrochromic device. As shown in Fig. 5, it comprises two polyester foils, one with a transparent and electrically conducting film of $\text{In}_2\text{O}_3:\text{Sn}$ (denoted ITO) and a superimposed tungsten oxide film, and another foil with ITO and superimposed nickel oxide. The oxide films are joined by a polymer electrolyte akin to the one discussed elsewhere [53]. The foil can be used for a variety of applications; the one in Fig. 5 refers to a specific type of “smart window” capable of combining indoor comfort and energy efficiency [18]. Practical manufacturing hinges on the development of a suitable process technology. Below we consider two aspects of this: materials capable of yielding a high bleached-state transmittance—as required for architectural applications [19]—and technology for in-line charge insertion/extraction in as-deposited electrochromic films.

3.1. Nickel oxide-based films with optimized bleached-state transmittance

The electrochromism in hydrated nickel oxide films containing Mg, Al, Si, V, Zr, Nb, Ag or Ta was investigated

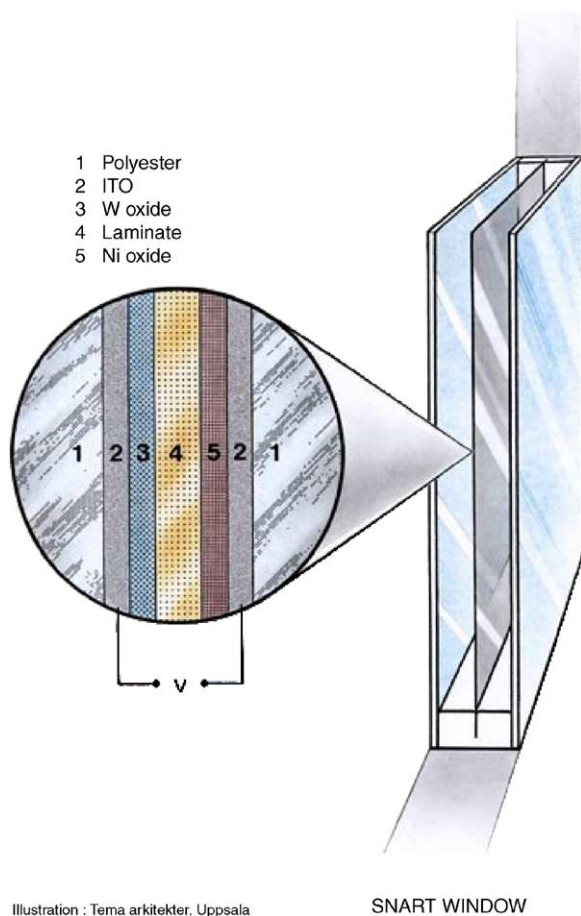


Illustration : Tema arkitekter, Uppsala

SMART WINDOW

Fig. 5. Schematic picture of an electrochromic foil suspended in a “smart window”.

recently with the objective of reducing the absorption in the visible range of the spectrum without compromising the electrochromic properties [41,54]. Films of different compositions were produced by co-sputtering. The sputtering power was varied until optimum electrochromic properties were found. The compositions of these films, which will be discussed in some detail below, were determined by Rutherford Backscattering Spectrometry (RBS) and can be represented by their atomic ratios between the additive and Ni according to $\text{Mg}/\text{Ni} = 0.80$ and $\text{Al}/\text{Ni} = 0.56\text{--}0.62$; the corresponding ratios of Si/Ni , Zr/Ni , Nb/Ni , Ag/Ni and Ta/Ni have not yet been determined. The sputter targets of the optimized compositions were non-magnetic or weakly magnetic, i.e., they were suitable for large-scale, large-area deposition.

Fig. 6 shows a cyclic voltammogram of nickel oxide and nickel–aluminum oxide in a KOH electrolyte. The shapes of the voltammograms change somewhat depending on the specific additive, but the main features characteristic for NiO tend to prevail. The charge capacity—and hence the magnitude of the electrochromism—is influenced by the potential-dynamic range, particularly the magnitude of the voltage for full coloration, U_{col} . It appears that similar charge capacities (from 15 to 20 mC/cm^2) can be obtained provided that U_{col} is varied by 0.05 to 0.1 V when additives are present. This shift is insignificant for electrochromic device applications. In general, irrespective of the additive it appears possible to produce electrochromic films with approximately the same electrochemical performance as for pure nickel oxide. This means that the main advantage of a mixed oxide lies in the improvement of the bleached-state optical properties, as discussed next.

Fig. 7 shows spectral absorbance $A(\lambda)$, calculated from measured transmittance T and reflectance R by

$$A(\lambda) = 1 - T(\lambda) - R(\lambda). \quad (3)$$

The data represent the bleached state for the various nickel-based oxides. A significant decrease of $A(\lambda)$ was found at short wavelengths for additives being Mg, Al, Si, Zr, Nb and Ta, whereas the films containing V and Ag did not show any improvement in their optical properties compared to those of pure nickel oxide. The results for Mg incorporation are consistent with those reported earlier by us [55]. One could note

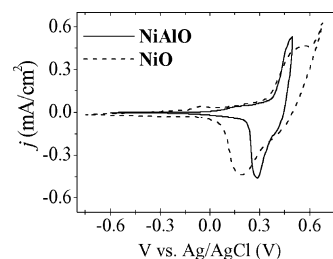


Fig. 6. Cyclic voltammogram (j - V) of nickel oxide and nickel–aluminum oxide films deposited from a single target. A scan speed of 10 mV s^{-1} was applied in a solution of 1 M KOH, using a three electrode cell.

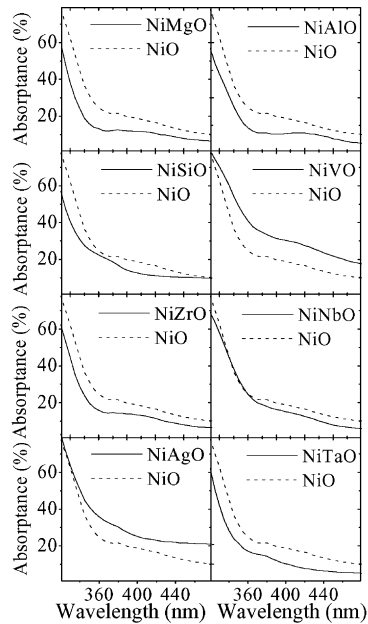


Fig. 7. Spectral absorbance of electrochromic nickel-oxide-based films in their bleached states. The designation NiXO (with X being Mg, Al, Si, V, Zr, Nb, Ag or Ta) indicates that X is present in the oxide but does not specify the amount.

that metals known to form oxides with wide band gaps tend to yield low bleached-state absorbance.

The strong absorbance at wavelengths below 350 nm is due to the semiconductor band gap, which appears to be widened as a consequence of the addition of Mg, Al, Si, Zr, Nb or Ta. On the other hand, the addition of V and Ag narrowed the band gap. Some weak absorption features can be discerned in the spectral data; they are possibly associated with charge transfer absorption [56]. Alternatively, the additives may affect optical absorption caused by defects such as vacancies, over-stoichiometry, grain boundaries, etc. Thermodynamically stable nickel oxide is a p-type conductor due to excess oxygen [57,58]. It is then plausible that the p-type conductivity and the residual optical absorption in the bleached state originate from the same electron states, and this may explain why films of pure nickel oxide cannot be made completely colorless. When Al is added, for example, it can act as a donor of electrons and fill the electron (hole) states on nickel, thereby reducing the residual absorption. The addition of vanadium, on the other hand, may provide acceptor states whose effect would be to enhance the residual absorption.

The perceived color is a very important property for architectural windows, including “smart” ones [19]. Quantitative assessments can be performed in several different ways, for example, by the CIE Colorimetric System [59,60]. Chromaticity coordinates for the various nickel-oxide-based films were calculated for four different standard illuminants representing a chosen set of light sources. Illuminant D65 signifies the average north sky daylight at 6500 K; illuminant A represents a tungsten halogen, incandescent light source at 2856 K (typical home or store accent lighting); illuminant

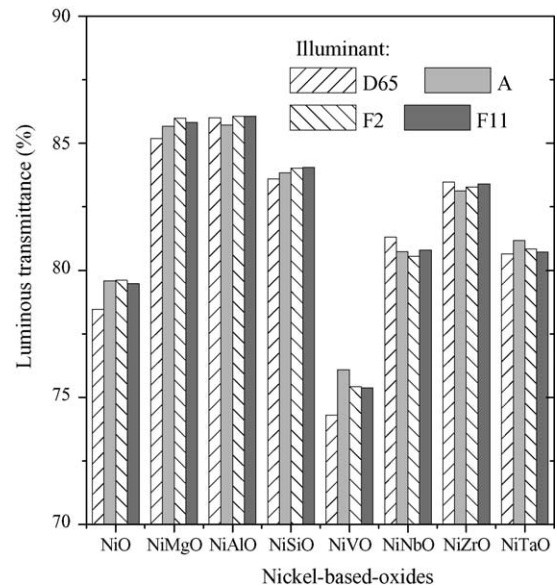


Fig. 8. Luminous transmittance for the nickel-oxide-based films reported on in Fig. 7 under four different CIE standard illuminants. The designation NiXO (with X being Mg, Al, Si, V, Zr, Nb, Ag or Ta) indicates that X is present in the oxide but does not specify the amount.

F11 pertains to a commercial, rare earth phosphor, narrow band fluorescent light source at 4000 K (used in Europe and the Pacific Rim for typical office or store lighting); and illuminant F2 represents a commercial, wide band fluorescent, cool white fluorescent light source at 4150 K (typical office or store lighting in the USA). One outcome of this analysis is the luminous transmittance, for which data are shown in Fig. 8. Films of nickel oxide mixed with Mg and Al show as much as 85% luminous transmittance, whereas films containing Si and Zr yield up to ~83%. For additives of Nb or Ta, the transmittance can be ~80%. The case of the vanadium admixture is different, though, and shows a luminous transmittance not exceeding 75%, i.e., lying ~4% below the value for pure nickel oxide. Generally speaking, the luminous transmittance shows a rather weak dependence on the specific illuminant. The results are entirely consistent with those in Fig. 7.

Data that are analogous with those presented above have been determined also for electrochromic iridium-oxide-based films. Specifically, additions of Mg and Al enhanced the bleached-state transmittance to ~83 or ~84% from the initial 79% of pure iridium oxide, while a tantalum-containing film had a luminous transmittance of ~82%. Zirconium, on the other hand, lowered the luminous transmittance by ~4% [61,62].

3.2. Pre-lamination charge insertion/extraction

With regard to manufacturing, it is preferable to be able to deposit the films under conditions that make them ready for device lamination or to have convenient processes for making the as-deposited films prepared for this. In the case of

tungsten oxide, one can carry out the deposition in a mixture of argon, oxygen and hydrogen according to principles described in the literature [63]. The hydrogen produces a blue color for the as-deposited films, and the key issue with regard to optimizing the gas mixture is to incorporate hydrogen into the film without creating major oxygen deficiency. In practice, the optimization of the tungsten oxide films can be made by measuring their color in the as-deposited state [9].

If nickel oxide films are to operate in conjunction with the tungsten oxide films the former, ideally, should be made so that they are prepared for charge insertion prior to device assembly. Such discharged films are dark. However, the nickel oxide films normally are transparent in their as-deposited state and hence require pre-treatment before device lamination. Charge insertion via an electrochemical procedure is possible, in principle, but obviously unwieldy and not suited for practical fabrication. An alternative method for discharging, as discussed next, employs exposure to ozone obtained by ultraviolet irradiation of the film in the presence of oxygen [64].

Fig. 9 displays the decrease of the luminous transmittance as a function of time when a conventional ozone photo-reactor was used to illuminate a nickel-oxide-based oxide film. The transmittance drops by some 50% during a few minutes, and a further decrease takes place for extended exposure times.

3.3. Device assembly

Polyester-based foils—one with a tungsten oxide film colored by sputtering in the presence of hydrogen and another with a nickel-oxide-based film colored by post-deposition ozone exposure—were laminated together by a polymer-based electrolyte using roll-pressing at a temperature of 80 °C. The edges of the double foil were then sealed, electrical contacts were attached and a electrochromic device—similar to the one outlined in Fig. 5—was ready for testing and use.

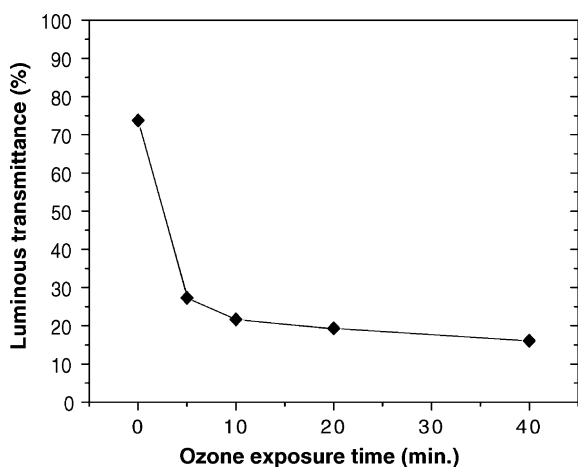


Fig. 9. Luminous transmittance vs. post-deposition ozone exposure time for a nickel–vanadium oxide film produced by sputtering in a mixture of argon, oxygen and hydrogen.

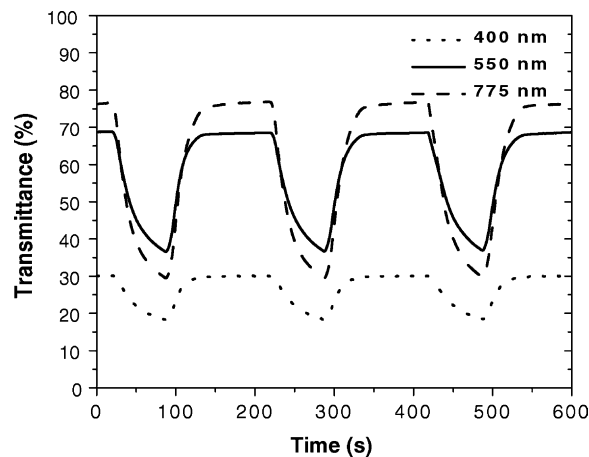


Fig. 10. Transmittance at three wavelengths vs. time for electrochromic switching of a laminated foil device.

Devices of this type were cycled between colored and bleached states using trapezoidal voltage pulses between -1.6 and $+1.5$ V, respectively. Fig. 10 shows transmittance at three different wavelengths for cycling with one full color/bleach cycle each 200 s. The optical modulation is pronounced, especially for mid-luminous and red light. Most of the changes take place within a few tens of seconds after application of the pulse, but the coloration has not reached saturation even after several minutes. Lower transmittance levels, down to 25% or considerably less in the colored state, could be reached for longer coloration times. It should be noted that the possibility of increasing the luminous transmittance by adding Al or Mg to the nickel oxide was not implemented for the investigations reported here. The devices have open circuit memory, which is an asset since electrical power must be drawn only to effect changes in the optical properties.

4. Applications

The work reported above has demonstrated techniques to produce flexible electrochromic foils with sufficient optical modulation range, dynamics, and durability for making them interesting for a number of applications. The largest and most challenging application—but also probably the most difficult one—lies in “smart windows”. It is important to realize that these windows can fulfill different goals: they can provide indoor comfort by being able to prevent glare and thermal stress, and simultaneously they can provide energy savings. The order of magnitude of the savings is considered next.

The solar energy falling onto a vertical surface per year is set to 1000 kWh/m². This can serve as a nominal value, whereas more correct numbers for south-facing/north-facing/horizontal surfaces are 850/350/920, 1400/450/1700 and 1100/560/1800 kWh/m² for Stockholm (Sweden), Denver (USA), and Miami (USA), respectively. Half of this, 500 kWh/m², is visible light. We use this number below since invisible (infrared) radiation can be reflected off—at least in

principle—by use of known technology that does not require variable transmittance. If the transparency can be altered between 7 and 75%—in accordance with some previous data [18]—the difference between having the window constantly colored and constantly bleached is 340 kWh/m^2 . But when should it be colored and when should it be bleached? With physical presence as the overriding control strategy, the question is when a room is in use—or, more precisely, the fraction of the solar energy that enters when nobody is present. Considering that a normal (office) room is empty during vacations, holidays and weekends, early mornings and late afternoons (when the sun is near the horizon), etc., it is surely a conservative estimate that 50% of the energy enters the room when there is no one to look through the window. Hence, this estimate yields that 170 kWh/m^2 is the amount of energy saved annually by adopting the given control strategy.

Is this energy savings significant or not? To answer this question, we note that today's best solar cell modules for regular use have an efficiency of 17%. Thus, they would be able to generate 170 kWh/m^2 in the example given above. Of course the analogy between energy savings in “smart windows” and energy generation in solar cells is not tied to the choice of the incident solar energy being 1000 kWh/m^2 but applies generally irrespectively of the orientation of the surface under examination. The “smart window” saves thermal energy, but if the cooling machine—operating with an efficiency of 300%, say—runs on electricity generated with an efficiency of 33% then the analogy becomes perfect. This latter consideration implies that we have a “national scenario” for the energy, with a “Coefficient-of-Performance” (“COP-factor”) equal to unity.

Buildings simulations were carried out recently with the object of providing realistic estimates of the energy savings inherent in the smart windows technology. Calculations for a standard office module with well-defined size, window area, lighting demand, occupancy, equipment, etc., showed that the energy savings potential was considerable for the cooling load. The considered office block was oriented with one façade facing South and one facing North and the simulations were performed with climate data from Rome (Italy), Brussels (Belgium), and Stockholm (Sweden). When using smart windows instead of static solar control windows, the annual cooling load could be reduced by as much as 40–50%. The amount of saved energy is obviously climate dependent. In moderately warm climates, such as Brussels and Stockholm, the number of days with very high outdoor temperature is relatively small. In such climates the cooling load generated by solar irradiation is fairly high, and an interesting result of the simulation work is that when smart windows were used, the cooling power could be reduced so that air conditioning systems could be completely avoided. In this case, the additional cost for smart windows hence can be more than compensated for by the elimination of an air conditioning system.

Potential applications in energy efficient architecture have provided the main impetus to a number of R&D efforts in Industry and Academia during the past several years. But there



Fig. 11. Electrochromics-based variable-transmittance visor for safe motorcycle riding.

are numerous other applications as well, a few having reached commercialization on a limited scale but most still in a development phase [65]. Specifically, “smart windows” are of great interest in vehicles and can be applied in various ways in cars, trucks, buses, trains, aircraft, etc. Variable-transmittance sunroofs in prestige cars are likely to be on the market soon. Automotive uses of automatically dimming “anti-dazzling” rear-view mirrors are in widespread use since several years; their technology is normally similar, though not identical, to the one discussed here. Applications are possible also in display devices of different kinds. For example, shelf labels, such as those used in supermarkets, can be devised so that they can show different prices at different times during the day thereby making it feasible to have hour-by-hour price discounts as a tool for optimizing customer flows.

Visors used on motorcycle helmets represent an interesting application for “smart foils”. These visors can be colored to a chosen degree in the day and bleached in the night. It is especially important that the driving and riding safety can

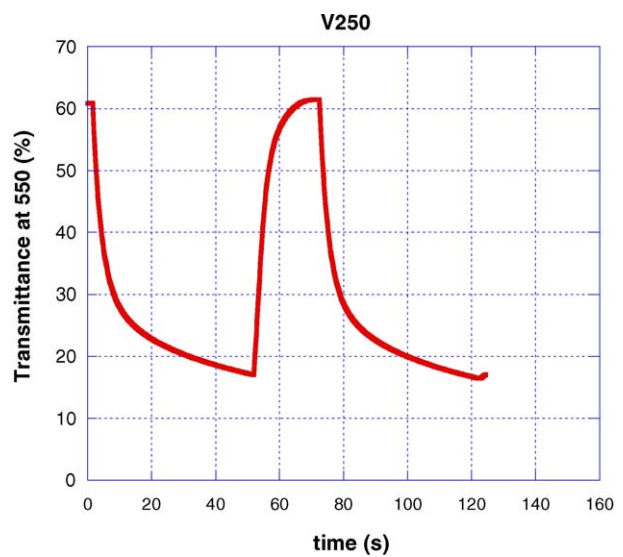


Fig. 12. Transmittance at a mid-luminous wavelength vs. time for electrochromic switching of a laminated foil device optimized for eyewear applications.

be significantly improved by having the visor bleach before entering tunnels or other dark spaces. Another aspect with a bearing on safety is that facial warming is limited by the visor's tint [66]. Fig. 11 shows a visor in bleached and colored state. Ski goggles, for example, have similar requirements, and Fig. 12 depicts the optical performance of a foil optimized for such applications. The list of potential applications can be extended almost at will.

5. Conclusions

Electrochromism was discovered and discussed in detail about 30 years ago [67], although still earlier observations of this phenomenon had been made [1]. A number of applications of electrochromism were in focus already from the beginning [68,69] but few of them have made it to the market. In general, high manufacturing costs and limited durability have been obstacles for the applicability of electrochromism. In this article, we have discussed flexible electrochromic foils, which have the potential for being produced by potentially inexpensive roll-to-roll technology. The foil is well suited for integration in a variety of applications such as eyewear and certain display devices. In a perspective of some years, we believe that the foils can be employed also in architectural “smart windows” capable of combining energy efficiency with improved indoor comfort.

The novel electrochromic foil includes thin films of tungsten oxide and nickel oxide and an intervening polymer electrolyte serving as lamination material. Concerning *scientific* aspects, we discussed the dominating defects in amorphous tungsten oxide and how they lead to a consistent picture of the optical properties of tungsten oxide films as a function of non-stoichiometry and ion intercalation. The same conceptual framework can encompass also the electrical properties [70]. We also presented a refined model for the coloration/bleaching due to proton extraction/insertion in surface sheaths of nano-crystallites of nickel oxide. Concerning *technology*, we treated ways to enhance the bleached-state transmittance by mixing the nickel oxide with another oxide having a wide band gap, pre-assembly charge insertion/extraction by facile gas treatments of the films, and practical device manufacturing. The final part of the paper covered *applications* with emphasis on architectural “smart windows”. We also touched upon applications concerning eyewear.

References

- [1] C.G. Granqvist, Handbook of Inorganic Electrochromic Materials, Elsevier, Amsterdam, The Netherlands, 1995.
- [2] C.G. Granqvist, Solar Energy Mater. Solar Cells 60 (2000) 201–262.
- [3] C.G. Granqvist, E. Avendaño, A. Azens, Thin Solid Films 442 (2003) 201–211.
- [4] C.M. Lampert, Solar Energy Mater. Solar Cells 76 (2003) 489–499.
- [5] S.-H. Lee, S.-K. Joo, Solar Energy Mater. Solar Cells 39 (1995) 155–166.
- [6] J.G.H. Mathew, S.P. Sapers, M.J. Cumbo, N.A. O'Brien, R.B. Sargent, V.P. Raksha, R.B. Lahaderne, B.P. Hichwa, J. Non-Cryst. Solids 218 (1997) 342–346.
- [7] A. Azens, L. Kullman, G. Vaivars, H. Nordborg, C.G. Granqvist, Solid State Ionics 113–115 (1998) 449–456.
- [8] A. Azens, G. Vaivars, M. Veszelei, L. Kullman, C.G. Granqvist, J. Appl. Phys. 89 (2001) 7885–7887.
- [9] A. Azens, G. Gustavsson, R. Karmhag, C.G. Granqvist, Solid State Ionics 165 (2003) 1–5.
- [10] R. Lechner, L.K. Thomas, Solar Energy Mater. Solar Cells 54 (1998) 139–146.
- [11] F. Michalak, K. von Rottkay, T. Richardson, J. Slack, M. Rubin, Electrochim. Acta 44 (1999) 3085–3092.
- [12] J. Nagai, G.D. McMeeking, Y. Saitoh, Solar Energy Mater. Solar Cells 56 (1999) 309–319.
- [13] A. Pennisi, F. Simone, G. Barletta, G. Di Marco, M. Lanza, Electrochim. Acta 44 (1999) 3237–3243.
- [14] C. Trimble, M. DeVries, J.S. Hale, D.W. Thompson, T.E. Tiwald, J.S. Woolam, Thin Solid Films 355–356 (1999) 26–34.
- [15] E.B. Franke, C.L. Trimble, J.S. Hale, M. Schubert, J.A. Woolam, J. Appl. Phys. 88 (2000) 5777–5784.
- [16] J. Karlsson, A. Roos, Solar Energy 68 (2000) 493–497.
- [17] K.-S. Ahn, Y.-C. Nah, J.-Y. Park, Y.-E. Sung, K.-Y. Cho, S.-S. Shin, J.-K. Park, Appl. Phys. Lett. 82 (2003) 3379–3381.
- [18] A. Azens, C.G. Granqvist, J. Appl. Electrochem. 7 (2003) 64–68.
- [19] M. Wigginton, Glass in Architecture, Phaidon, London, UK, 1996.
- [20] A. Campagno, Intelligente Glasfassaden/Intelligent Glass Façades, fifth ed., Birkhäuser, Basel, Switzerland, 2002.
- [21] G.A. Niklasson, L. Berggren, A.-L. Larsson, Solar Energy Mater. Solar Cells 84 (2004) 315–328.
- [22] A. Hjelm, C.G. Granqvist, J.M. Wills, Phys. Rev. B 54 (1996) 2436–2454.
- [23] C. Bechinger, M.S. Burdis, J.G. Zhang, Solid State Commun. 101 (1997) 753–756.
- [24] J.-G. Zhang, D.K. Benson, C.E. Tracy, S.K. Deb, A.W. Czanderna, C. Bechinger, J. Electrochem. Soc. 144 (1997) 2022–2026.
- [25] S.-H. Lee, H.M. Cheong, C.E. Tracy, A. Mascarenhas, A.W. Czanderna, S.K. Deb, Appl. Phys. Lett. 75 (1999) 1541–1543.
- [26] G.A. de Wijs, R.A. de Groot, Phys. Rev. B 60 (1999) 16463–16474.
- [27] M. Stoltze, B. Camin, F. Galbert, U. Reinholz, L.K. Thomas, Thin Solid Films 409 (2002) 254–264.
- [28] G.A. de Wijs, R.A. de Groot, Electrochim. Acta 46 (2001) 1989–1993.
- [29] P.W. Anderson, Phys. Rev. Lett. 34 (1975) 953–955.
- [30] T.J. Vink, E.P. Boonekamp, R.G.F.A. Verbeek, Y. Tamminga, J. Appl. Phys. 85 (1999) 1540–1544.
- [31] A.S. Foster, V.B. Sulimov, F.L. Gejo, A.L. Schluger, R.M. Nieminen, Phys. Rev. B 64 (2001) 224108–224110.
- [32] L. Berggren, A. Azens, G.A. Niklasson, J. Appl. Phys. 90 (2001) 1860–1863.
- [33] L. Berggren, G.A. Niklasson, Solid State Ionics 165 (2003) 51–58.
- [34] B.W. Faughnan, R.S. Crandall, P.M. Heyman, RCA Rev. 36 (1975) 177–197.
- [35] V.V. Bryksin, Fiz. Tverd. Tela 24 (1982) 1110–1117 [English translation Soviet Phys. Solid State 24 (1982) 627–631].
- [36] J.V. Gabrusenoks, P.D. Cikmach, A.R. Lulis, J.J. Kleperis, G.M. Ramans, Solid State Ionics 14 (1984) 25–30.
- [37] H. Kaneko, K. Miyake, Y. Teramoto, J. Appl. Phys. 53 (1982) 4416–4421.
- [38] M.S. Burdis, J.R. Siddle, Thin Solid Films 237 (1994) 320–325.
- [39] E. Masetti, M.L. Grilli, G. Dautzenberg, G. Macrelli, M. Adamik, Solar Energy Mater. Solar Cells 56 (1999) 259–269.
- [40] M. Denesuk, D.R. Uhlmann, J. Electrochem. Soc. 143 (1996) L186–L188.

- [41] E. Avendaño, A. Azens, G.A. Niklasson, C.G. Granqvist, in: A. Rougier, D. Rauh, G.A. Nazri (Eds.), *Electrochromic Materials and Applications*, vol. PV 2003-17, The Electrochemical Society, Pennington, USA, 2003, pp. 80–90.
- [42] E. Avendaño, A. Azens, G.A. Niklasson, C.G. Granqvist, submitted for publication.
- [43] E. Avendaño, A. Azens, G.A. Niklasson, C.G. Granqvist, submitted for publication.
- [44] E. Avendaño, A. Azens, J. Isidorsson, R. Karmhag, G.A. Niklasson, C.G. Granqvist, *Solid State Ionics* 165 (2003) 169–173.
- [45] E. Avendaño, A. Azens, G.A. Niklasson, C.G. Granqvist, *J. Solid State Electrochem.* 8 (2003) 37–39.
- [46] E. Avendaño, A. Kuzmin, J. Purans, A. Azens, G.A. Niklasson, C.G. Granqvist, *Phys. Scripta*, submitted for publication.
- [47] G.R. Rao, M.S. Hegde, D.D. Saema, C.N.R. Rao, *J. Physics: Condensed Matter* 1 (1989) 2147–2150.
- [48] J.F. Moulder, W.F. Stickle, P.E. Sobol, K.D. Momben, *Handbook of X-ray Photoelectron Spectroscopy*, Physical Electronics, Minnesota, USA, 1995.
- [49] A.N. Mansour, *Surface Sci. Spectra* 3 (1996) 231–239.
- [50] A.N. Mansour, C.A. Melendres, *Surface Sci. Spectra* 3 (1996), pp. 247, 255, 263, 271.
- [51] L.M. Moroney, R.S.C. Smart, M.W. Roberts, *J. Chem. Soc.: Faraday Trans. I* 79 (1983) 1769–1778.
- [52] P.A. Cox, *The Electronic Structure and Chemistry of Solids*, Oxford University Press, Oxford, UK, 1998.
- [53] W. Wixwat, J.R. Stevens, A.M. Andersson, C.G. Granqvist, in: B. Scrosati (Ed.), *Second International Symposium on Polymer Electrolytes*, Elsevier Applied Science, London, UK, 1990, pp. 461–465.
- [54] E. Avendaño, A. Azens, G.A. Niklasson, C.G. Granqvist, *Solar Energy Mater. Solar Cells* 84 (2004) 337–350.
- [55] A. Azens, J. Isidorsson, R. Karmhag, C.G. Granqvist, *Thin Solid Films* 422 (2002) 1–3.
- [56] T.M.J. Nilsson, G.A. Niklasson, *Proc. Soc. Photo-Opt. Instrum. Eng.* 1272 (1990) 129–138.
- [57] D. Adler, J. Feinleib, *Phys. Rev. B* 2 (1970) 3112–3134.
- [58] P. Lunkenheimer, A. Loidl, C.R. Ottermann, K. Bange, *Phys. Rev. B* 44 (1991) 5927–5930.
- [59] D.L. MacAdam, *Color Measurement: Theme and Variations*, Springer, Berlin, Germany, 1981.
- [60] S.J. Williamson, H.Z. Cummins, *Light Color in Nature and Art*, Wiley, New York, USA, 1983.
- [61] A. Azens, C.G. Granqvist, *Appl. Phys. Lett.* 81 (2002) 928–929.
- [62] J. Backholm, A. Azens, G.A. Niklasson, submitted for publication.
- [63] A.P. Giri, R. Messier, *Mater. Res. Soc. Symp. Proc.* 24 (1984) 221–227.
- [64] A. Azens, L. Kullman, C.G. Granqvist, *Solar Energy Mater. Solar Cells* 76 (2003) 147–153.
- [65] C.M. Lampert, *Mater. Today* (3) (2004) 28–35.
- [66] M. Buyan, P.A. Brühwiler, A. Azens, G. Gustavsson, R. Karmhag, C.G. Granqvist, submitted for publication.
- [67] S.K. Deb, *Philos. Mag.* 27 (1973) 801–822.
- [68] S.K. Deb, *Proc. Soc. Photo-Opt. Instrum. Eng.* 692 (1986) 19–31.
- [69] S.K. Deb, *Solar Energy Mater. Solar Cells* 25 (1992) 327–338.
- [70] J. Ederth, A. Hoel, G.A. Niklasson, C.G. Granqvist, *J. Appl. Phys.* 96 (2004) 5722–5726.